Simplifying Electron Diffraction Pattern Identification of Mixed-Material Nanoparticles

Jacopo Samson,[1] Patrick C. Nahirney,[2] Charles Michael Drain,[1] and Irene Piscopo[3] *
[1]Department of Chemistry, Hunter College, 695 Park Avenue, New York, NY 10065
[2]Division of Medical Sciences, University of Victoria, Victoria, BC V8W 2Y2, Canada
[3]EM Consulting, 57 Soundview Drive, Huntington, NY 11743
* irene.piscopo@gmail.com

Introduction

Metallic and non-metallic nanoparticles (NPs), ranging in size from 1–200 nm, have unique functional properties that differ from their bulk materials and their component atoms or molecules [1]. These unique properties have driven the demand for nano-sized materials and new methods to synthesize NPs, which are used in drug delivery systems [2], bio-imaging agents [3], catalysts [4], photonics, and optical devices [5]. Inorganic NPs can be synthesized with a variety of methods that impart size, shape, and other structural properties. Cobalt-based NPs, for instance, display unique size and shape-dependent magnetic properties [6], while the band gap, UV blocking properties and stability of zinc oxide (ZnO) NPs enable new applications in products ranging from cosmetics [7] to solar cell power [8].

Approaches to NP synthesis include solvothermal, biological, and other templates [9], as well as ligands to seed NP growth and molding strategies [10]. Our approach for synthesizing metal NPs involves using toroidal topologies of plasmid DNA as sacrificial molds and varying conditions to fabricate size-tunable gold, nickel, and cobalt NPs [9]. Plasmid DNA provides a relatively inexpensive monodispersed template that can be engineered to form in a range of sizes and exploits the well-established high affinity for metal cations. This strategy is generally a greener approach to NP synthesis because the solvent is water and the template is biodegradable.

We have characterized these NPs by atomic force microscopy (AMF) and transmission electron microscopy (TEM). For example, a pcDNA3.1 (+) plasmid can be used as a sacrificial mold to yield disc-shaped gold and nickel NPs in the range of 28 ± 3 nm × 8 ± 1 nm and 52 ± 5 nm × 13 ± 1 nm, respectively. Columnar-shaped ZnO NPs were synthesized using a pH gradient and imaged to reveal a bimodal distribution in the range of 70 ± 10 nm × 50 ± 10 nm and 135 ± 15 nm × 80 ± 10 nm. In order to confirm the nature of these NPs, which were composed of both metals and non-metallic materials, we compared their electron microdiffraction (μD) patterns to known standards [11–12].

There are two methods for obtaining electron diffraction (ED) patterns [13]. The selected area diffraction (SAD) method uses an aperture to select the area producing the ED pattern, while μD and convergent beam electron diffraction (CBED) techniques use the beam to select the area producing the pattern. The minimum area that can be selected on a 100 kV TEM by the SAD method is 1 μ [12]. Because μD uses the beam to select the area, the minimum size in the TEM mode is limited by the electron source. The sharp diffracted beams of μD, as opposed to the discs of CBED, are produced by using a small (20–30 μ) second condenser aperture [14]. Because the size of the NPs under examination was less than 200 nm, μD was the method of choice.

Microdiffraction (μD) is a reliable method of verifying the identity of individual NPs when there is not enough sample for powder X-ray diffraction (XRD) analysis. In the use of plasmid molds, the resulting materials could be the starting metal ion salts, the metal oxides, the target metal NPs, or combinations of these (for example, nickel metal, NiO, Ni_2O_3, NiX_2). Similar analytical criteria are needed for the formation of inorganic materials such as ZnO and TiO_2. Morphology alone cannot differentiate these NPs because the metals in the NPs sometimes exist in more than one oxidation state. In other cases, similar morphologies proved to be two different materials. Identification of the NPs necessitated the indexing of individual diffraction patterns, a very time consuming and tedious procedure.

To simplify the identification of materials, when one has an idea what the material might be (that is, NiO or Ni_2O_3) and standards with which to compare them, we present two easily applied and straightforward methods for comparing electron diffraction (ED) patterns. Identifying total unknowns will still require indexing individual diffraction patterns. The example shown in Figure 1 illustrates that this technique can be applied to inclusions in tissue samples as well as to particulate materials.

Materials and Methods

Materials. Me_3PAuCl and $Co(II)Cl_2 \cdot 6H_2O$ were purchased from Sigma Aldrich, and $Ni(II)Cl_2 \cdot 6H_2O$ was purchased from Fisher Scientific. The pcDNA3.1(+) plasmid was obtained from Invitrogen, amplified with Qiagen kit to a mother stock suspension of 1 mg/mL and diluted when mixed with the cationic-containing solutions. The 12 mM stock solutions of metal chlorides were prepared in nanopure water. The gold solution was prepared by adding an equal portion of deionized water to 100 mL of a 24 mM stock solution of Me_3PAuCl dissolved in acetone. $Zn(NO_3)_2 \cdot 6H_2O$ (Sigma Aldrich) was dissolved in deionized water at a concentration of 50 mM. Tris (Sigma Aldrich) was prepared in deionized water at a concentration of 100 mM. Tris-EDTA (TE) buffer (10 mM Tris, 1 mM EDTA, pH 8) was included in the Qiagen kit.

Instrumentation. Samples for TEM observation and μD were dispersed onto carbon-coated copper grids (Electron Microscopy Sciences). The samples were imaged and the μD patterns collected at 120 kV using a Tecnai G2 Biotwin (FEI). All images and μD patterns were collected with an AMT 2K CCD camera.

We obtained μD patterns of known standards and then, under the same conditions (kV and camera length), we obtained μD patterns of the unknowns. For both methods to

https://doi.org/10.1017/S1551929511001179 Published online by Cambridge University Press

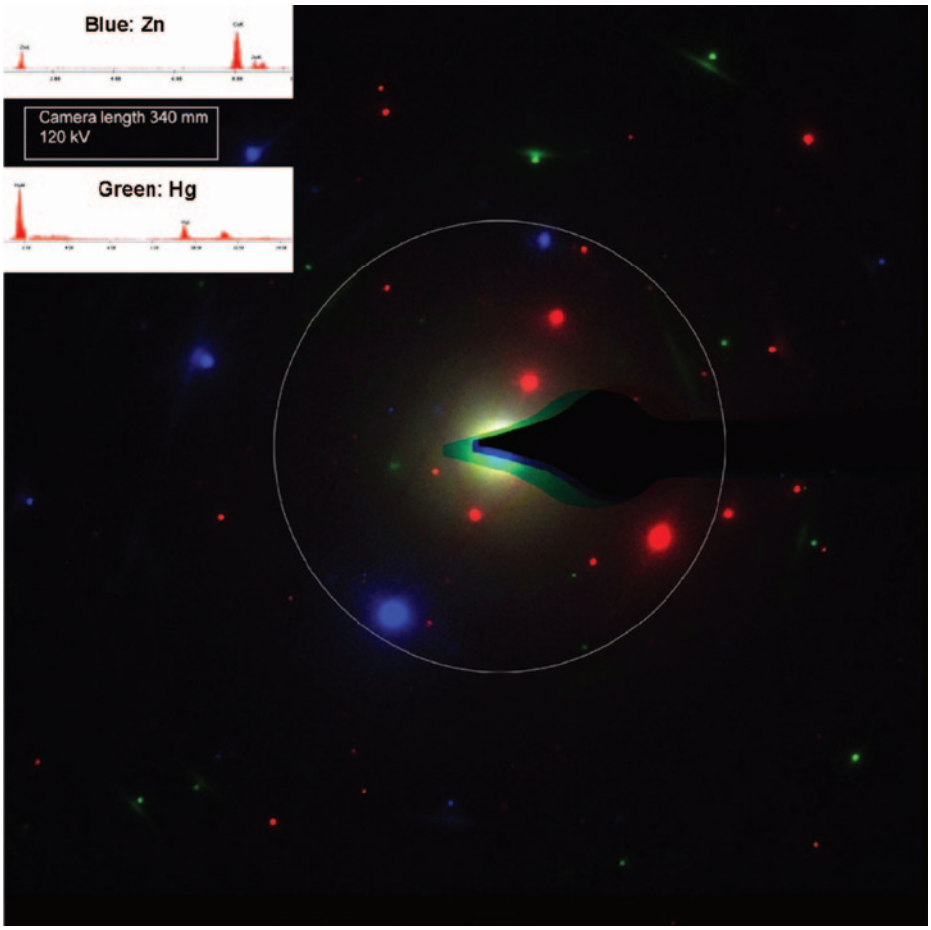

Figure 1: Microdiffraction (μD) patterns of a known material (TiO_2, red) and two unknown nanoparticles (NPs) from a colored tattoo (blue: Zn; green: Hg) collected at the same kV and camera length (120 kV and 340 mm). EDS spectra of Zn and Hg are shown in the inserts on the top-left corner. Using the colorized image overlay method and rotating the images relative to one another, no matching patterns could be identified. The white circle was inscribed to help center the beam stop. The blue dots, representing two diffracted beams from the same diffraction ring, are equidistant from the central spot. When the beam stop is correctly positioned, then the two blue diffracted beams are equidistant from the white circle.

work successfully, one must ensure that both the standard and the unknown are in the eucentric position for both imaging and diffraction pattern acquisition. This ensures accurate camera length comparisons. Images of the μD patterns were saved as TIFF files for data comparison in Adobe Photoshop, where the diffraction patterns were colorized and superimposed using the layer palette.

Results and Discussion

Method 1: After collecting the diffraction patterns, they were pseudo-colored in Adobe Photoshop, and these colorized patterns were overlaid for direct comparison. This simple technique requires only the superimposition of the μD pattern of the standard metal or non-metal with the experimental pattern of the analyzed sample of interest. In order to obtain an accurate and reproducible superimposition, the patterns must be collected under the identical conditions discussed above and within relatively close time frames. By overlaying the patterns, we obtained instant and distinct matches or mismatches. Diffraction patterns considered as mismatches were patterns that contained extraneous d-spacings that were not present in the standards.

In Figure 1 three NPs of distinctly different known materials are compared (red: rutile TiO_2; green: mercury; blue: zinc). This illustrates non-overlapping μD patterns. There is the possibility, when using spot patterns, that such non-overlapping spot patterns could be from the same material, but these diffraction patterns were taken of differently oriented particles. In our case the particle differences were also confirmed by energy-dispersive X-ray spectrometry (EDS). Ring patterns, which are usually produced from many differently oriented particles, eliminate this ambiguity. Indeed, when there are numerous particles, the discrete diffracted beams combine to form a continuous ring, as shown in Figure 3A, as compared to Figure 4 where fewer NPs are producing the μD patterns; therefore, individually diffracted beams are visible.

Overlaying these colorized diffraction patterns in Photoshop allows for rapid screening of samples, by matching diffraction patterns to known standards or seeing definitive differences. Figures 2C and 3C show matching diffraction patterns of an unknown and known material. This is an effective way to rapidly verify if the identity of the unknown matches the standard and may be applicable as an analytical tool for the quality control of production batches of nanomaterials and/or biological-related materials (see skin tattoos shown in Figure 1). Using this method, we have successfully identified the metal properties of plasmid DNA-molded nanodiscs of gold (Figure 2) and nickel nanoparticles (Figure 3). We were able to vary conditions to fabricate size tunable gold and nickel, and ensure by this method, that we were maintaining the same material.

Method 2: A μD pattern from a standard of ZnO powder on a carbon-coated grid was collected and printed on an overhead transparency. The transparency was then overlaid onto the standard μD pattern on the CCD monitor to check if any distortion of the μD pattern occurred when printing onto the transparency. To compare a μD pattern from an unknown to the standard, the transparency was overlaid on the unknown diffraction pattern directly on the CRT monitor of the AMT camera. Diffraction patterns considered as mismatches were patterns that contained extraneous d-spacings from those in the standards. To be considered a match to the standard, the μD pattern on the CRT had to match with at least five of the standard's d-spacings.

As the synthesis processing was refined, and μD confirmed the homogeneous nature of the desired NPs, this method

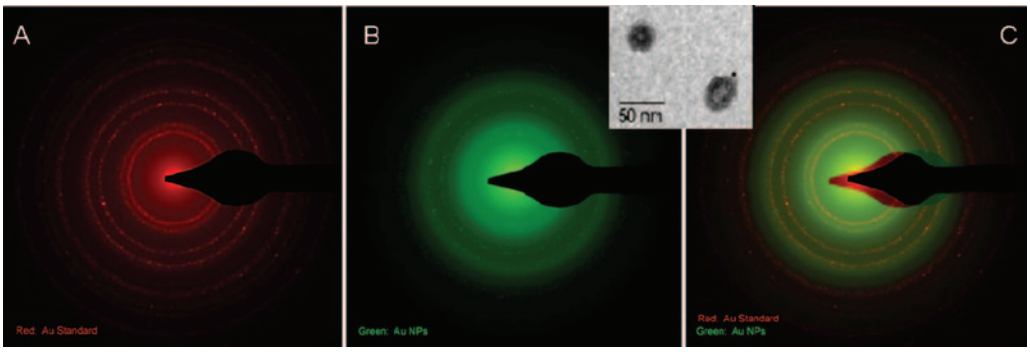

Figure 2: (A) A μD ring pattern from an evaporated gold standard. (B) A μD pattern of several gold particles prepared using toroidal DNA to control the size. (C) Superimposition of gold standard A and identified unknown B. The TEM image (insert) shows the toroidal DNA/gold formation. Note that the inner, more intense rings, when superimposed, become yellow whereas the outer, less intense rings maintain their original color.

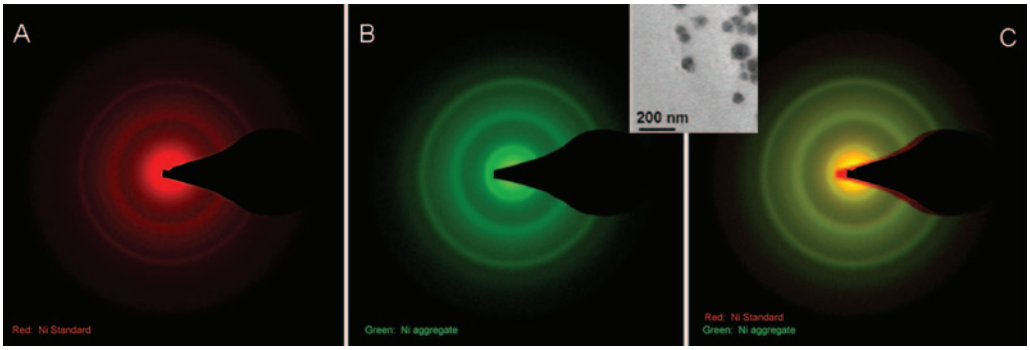

Figure 3: (A, red) A μD pattern from an evaporated nickel standard. (B, green) A μD pattern from an aggregate of Ni NPs. (C) Superimposition of nickel standard A and identified unknown B. The TEM image (insert) shows the Nickel NP formation upon DNA mold degradation. When there are numerous particles, the discrete diffracted beams combine to form a continuous ring as compared to Figure 4 where fewer NPs are producing the μD patterns.

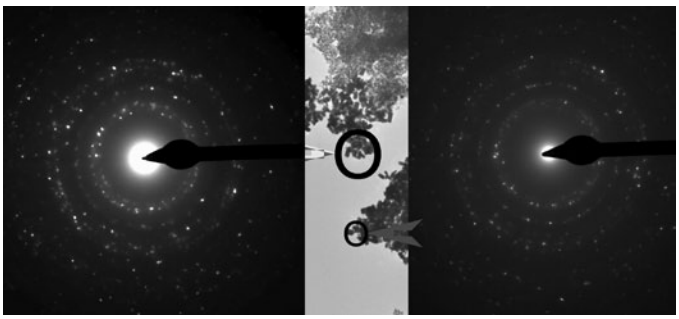

Figure 4: μD pattern images displayed on a monitor corresponding to unknown NP aggregates that were identified as ZnO by Method 2 (overhead transparency method).

allowed us to check the results and make a rapid assessment and adjustment to our synthesis within the time frame of a couple of hours. This method is the easier of the two methods for comparison of standard selected area diffraction (SAD) patterns or large area μD patterns where ring patterns are formed.

Conclusion

A full match of the superimposed standard and experimental unknown μD patterns by both digital image overlay and overhead transparency methods allow us to obtain a swift and accurate determination of the nature of the material investigated without tedious indexing of individual diffraction patterns as long as standards are available. To ensure accuracy of these comparisons, it is essential that the same conditions be used to obtain the diffraction patterns to be compared (that is, kV, camera length, and specimen height). This ensures accurate comparisons.

Methods 1 and 2 will work even when only milligrams or micrograms of material is available, for example when analyzing NPs formed in microfluidic reactors [15]. The methods described herein (that is, μD where the beam is used to select the area) can be used on any TEM and is especially useful on those TEMs not equipped with a SAD aperture.

Acknowledgments

We thank Alexander Yampolsky for his help in sample preparation and Dr. H. Amalia Pasolli at Rockefeller University for allowing us to use her Tecnai TEM for this work after Patrick C. Nahirney left Rockefeller University for Victoria, BC, Canada. This work was supported by NSF grants to CMD (CHE-0847997). Hunter College science infrastructure is supported by the National Science Foundation, the National Institutes of Health including the RCMI program (G12-RR-03037), and the City University of New York.

References

[1] AP Alivisatos, *Science* 271 (1996) 933–37.
[2] F Stellacci, *Nature Materials* 4 (2005) 113–14.
[3] P Sharma et al., *Chem Mater* 20 (2008) 6087–94.
[4] A Wieckowski et al., *Catalysis and Electrocatalysis at Nanoparticle Surfaces*, Marcel Dekker, New York, 2003.
[5] M Grzelczak et al., *ACS Nano* 4 (2010) 3591–3605.
[6] Q Song, *J Am Chem Soc* 126 (2004) 6164–68.
[7] SE Cross et al., *Skin Pharmacol Physiol* 20 (2007) 148–54.
[8] W Beek et al., *J Mater Chem* 15 (2005) 2985–88.
[9] J Samson et al., *ACS Nano* 3 (2009) 339–44.
[10] O Masala et al., *Ann Rev Mater Research* 34 (2004) 41–81.
[11] JJ Bozzola and LD Russell, *Electron Microscopy*, Jones and Bartlett Publishers, Boston, 1992, 347–55.
[12] BEP Beeston, RW Horne, and R Markham, *Electron Diffraction and Optical Diffraction Techniques*, Elsevier Science Ltd., Amsterdam and New York, 1994.
[13] A Eades, *Microscopy Today*, 19(1) (2011) 72.
[14] JW Steeds, in *Introduction to Analytical Electron Microscopy*, Plenum Press, New York, 1979, ch. 15, 390.
[15] Y Song et al., *Chem of Mater* 18 (2006) 2817–27.

MT